Degradation of permafrost beneath a road embankment enhanced by heat advected in groundwater[1]

Isabelle de Grandpré, Daniel Fortier, and Eva Stephani

Abstract: For the past few decades, northwestern North America has been affected by climate warming, leading to permafrost degradation and instability of the ground. This is problematic for all infrastructure built on permafrost, especially roads and runways. Thaw settlement and soil consolidation promote embankment subsidence and the development of cracks, potholes, and depressions in road pavement. In this study, we investigate highway stability in permafrost terrain at an experimentally built road embankment near Beaver Creek, Yukon. A network of 25 groundwater monitoring wells was installed along the sides of the road to estimate groundwater flow and its thermal impact on the permafrost beneath the road. Data on topography, water-table elevation, ground temperature, and stratigraphy of the soil were collected at the site. The geotechnical properties of each soil layer were determined by laboratory analysis and used to calibrate a two-dimensional groundwater flow model. Field observations showed that water was progressively losing heat as it flowed under the road embankment. Our results suggest that advective heat transfer related to groundwater flow accelerated permafrost degradation under the road embankment.

Résumé : Le secteur nord-ouest de l'Amérique du Nord est affecté depuis quelques décennies par les changements climatiques, entraînant une dégradation du pergélisol et une déstabilisation de la surface du sol. Ceci est problématique pour les infrastructures bâties sur le pergélisol, particulièrement les routes et les pistes d'atterrissages. Le tassement au dégel et la consolidation subséquente du sol dégelé entraînent une subsidence des remblais et la formation de fissures, de nids-de-poule et de dépressions dans la route. Afin d'étudier la stabilité des infrastructures routières en milieu de pergélisol, un tronçon expérimental de route à remblais a été construit près de Beaver Creek, Yukon. Un réseau de 25 puits d'observation a été installé de part et d'autre de la route au site d'étude afin d'estimer le potentiel d'écoulement d'eau sous la route ainsi que l'impact thermique de cet écoulement sur le pergélisol. Des données de topographie, d'élévation de la nappe phréatique, de température du sol et de stratigraphie ont été prises au site d'étude. Les propriétés géotechniques de chaque couche de sol ont été déterminées par des analyses de laboratoire et ont été utilisées pour calibrer un modèle 2D d'écoulement souterrain. Les observations de terrain ont démontré que l'eau perdait progressivement de sa chaleur à mesure qu'elle s'écoulait sous la route. Nos résultats suggèrent que des transferts de chaleur convectifs relatifs à l'écoulement souterrain aient contribué à l'accélération de la dégradation du pergélisol sous la route.

Introduction

Warming of permafrost due to increasing air temperature has been observed in northwest North America for several decades (Osterkamp and Romanovsky 1999; Osterkamp 2005; Smith et al. 2010). In Alaska, subsidence and expansion of surface water bodies have been associated with permafrost degradation due to such climate change (Pullman et al. 2007). The principal effects of climate warming on permafrost are increases in ground temperature and active-layer thickness, and development of taliks.

Northern transportation infrastructure, especially roads and runways, is sensitive to permafrost degradation (Jin et al. 2006). Melting of ground ice and thaw consolidation promote embankment subsidence and the development of cracks, potholes, and depressions in the road pavement (Qingbai et al. 2002*b*; Fortier and Bolduc 2008; Stephani et al. 2010). Permafrost warming induced by climate change can be amplified

Received 9 July 2011. Accepted 29 March 2012. Published at www.nrcresearchpress.com/cjes on 29 May 2012.

Paper handled by Associate Editor Chris R. Burn.

I. de Grandpré. Département de Géographie, Université de Montréal, 520 Chemin Côte-Sainte-Catherine, Montréal, QC H2V 2B8, Canada; Centre d'études nordiques, Université Laval, Québec, QC, Canada.
D. Fortier. Département de Géographie, Université de Montréal, 520 Chemin Côte-Sainte-Catherine, Montréal, QC H2V 2B8, Canada; Centre d'études nordiques, Université Laval, Québec, QC, Canada; Institute of Northern Engineering, University of Alaska Fairbanks, Fairbanks, AK, USA.
E. Stephani. Centre d'études nordiques, Université Laval, Québec, QC, Canada; Institute of Northern Engineering, University of Alaska Fairbanks, Fairbanks, AK, USA; Department of Civil and Environmental Engineering, University of Alaska Fairbanks, Fairbanks, AK, USA.

Corresponding author: Isabelle de Grandpré (e-mail: Isabelle.de.grandpre@umontreal.ca).

[1]This article is one of a series of papers published in this CJES Special Issue on the theme of *Fundamental and applied research on permafrost in Canada*.

Fig. 1. Example of depressions observed at the central line of the road in early June. The depression was 1 m wide and 10 cm deep.

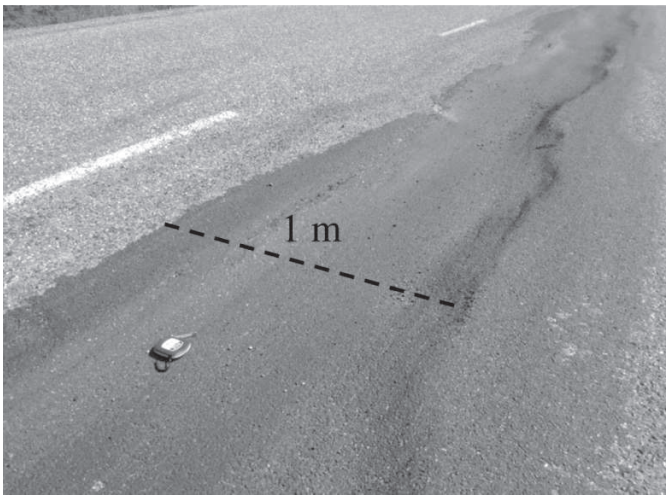

by construction operations (e.g., soil compaction, destruction of the vegetation cover), embankment geometry, snow accumulation on side slopes, or changes in material properties, such as the normally low albedo of pavement surfaces (Qingbai et al. 2002*a*; Kondratiev 2008). Road degradation presents problems due to the high costs of construction and maintenance, and because driving conditions may become hazardous (Nelson et al. 2002; Remchein et al. 2009).

Permafrost degradation also affects the groundwater flow regime. Groundwater flow in permafrost terrain is controlled by factors such as soil texture, ice content, and configuration (cryostructure; Egginton and Dyke 1990; Jorgenson et al. 2001; Quinton et al. 2005; Woo et al. 2008). Flow is usually confined to the active layer and other unfrozen ground (Woo et al. 2008). Consequently, as permafrost degrades, new groundwater flow paths may be created. Drainage of peatlands and lakes and acceleration of thermokarst processes have all been reported following increases in groundwater flow (Hinzman et al. 2005).

Linear transportation infrastructure commonly intersects the natural drainage network. Culverts are usually inserted in embankments to drain the main streams, and bridges are built for river crossings. Under low flow conditions, porous embankment materials and multiple culverts have been used successfully to enable water flow through a structure, with minimal modification to flow patterns (McGregor et al. 2010). However, groundwater flow paths in permafrost terrain are often hard to predict and rarely taken into account in the design of embankments.

Field observations and measurements along a road transect in discontinuous permafrost near Beaver Creek, Yukon, between 2008 and 2010 showed an acceleration of road subsidence under the centerline of the road where groundwater flow was suspected (Fig. 1). At this location, the road subsided at a rate of about 10 cm/month between June and October. This paper investigates whether accelerated thawing of the active layer and near-surface permafrost was caused by heat transferred from groundwater to the frozen embankment and natural ground. Advective heat transfer may be an order of magnitude more important than conductive heat transfer in the embankment (Kane et al. 2001), yet remains poorly understood and quantified in permafrost environments.

The objectives of this paper are to (*i*) estimate groundwater flow in an ice-rich discontinuous permafrost setting, (*ii*) measure water temperature in the ground and under the road embankment, and (*iii*) model seepage dynamics within and under the road.

Study site

The study site is a segment of the Alaska Highway, located in ice-rich discontinuous permafrost near Beaver Creek, Yukon (62°20′N, 140°50′W; Rampton 1971; Scudder 1997; Fig. 2*a*). The climate of the region is continental, with long, cold winters and short, dry summers (Scudder 1997; Ogden 2006). The mean annual air temperature is –5.5 °C; only 4 months of the year have a mean air temperature above 0 °C. The mean annual precipitation is 416 mm (Environment Canada 2002). Snowfall begins annually in September, and snowmelt begins in April. The vegetation is taiga, with stunted spruce, shrubs, tussocks, and mosses (Scudder 1997).

The site is located in a former silty floodplain in which sediments have been reworked by slopewash and colonized by vegetation. The road segment investigated in this paper was built between 1994 and 1996 about 100 m from the old alignment in a northwest–southeast orientation (Fig. 2). The road is aligned sub-perpendicularly to the local slope. Since its construction, the centerline of the road has subsided due to degradation of the underlying ice-rich permafrost. The embankment crosscuts the natural drainage network. Excavations in April 2008 to remove berms on the side of the road exposed saturated taliks in the embankment material and the fine-grained sediments beneath the road (Stephani et al. 2008).

Methods

Water-table characterization

A network of 25 standpipes to measure the elevation of the water table was installed in an area of about 10 000 m^2, where interpretation of satellite image and field observations suggested groundwater flow under the road (Fig. 2B). On each side of the road, two rows of groundwater monitoring wells were installed: one in undisturbed ground, and one at the edge of the embankment in a mixture of embankment material and silt (Figs. 3, 4). The standpipes were installed in October 2008 to between 30 and 85 cm below the ground surface, near the base of the active layer. Six pore-water pressure and temperature sensors (Onset Hobo U20-001-01 water level loggers, Onset Computer Corporation, Bourne, Massachusetts) were installed in the standpipes, where concentrated groundwater flow was suspected. These sensors were installed 7 cm above the bottom of the groundwater wells to record water pressure and temperature data every hour, with an accuracy of 0.05 kPa (5 mm) and 0.4 °C. In-ground hydrostatic pressures were corrected for variations in atmospheric pressure measured on site. After correction, hydrostatic pressures were converted to water level (centimetres of water in well). Water-table elevations and temperatures were measured manually between October 2008 and September 2010 to corroborate automatically collected data. Water elevations were imported in SIGIS software (Daoust

Fig. 2. Location of the study site (62°20′N, 140°50′W). (A) Map of Yukon Territory, Canada (modified from Natural Resources Canada 2006). (B) Satellite image (QuickBird, DigitalBorbe, Longmont, Colorado) of the study site, 14 June 2006. 1, Inset: groundwater measurement location (groundwater monitoring wells and pressure sensors); 2, Alaska Highway; 3, former Alaska Highway alignment; 4, stream; 5, the line shows an area with a vegetation pattern (lighter gray) aligned with the supposed direction of groundwater flow (white arrow).

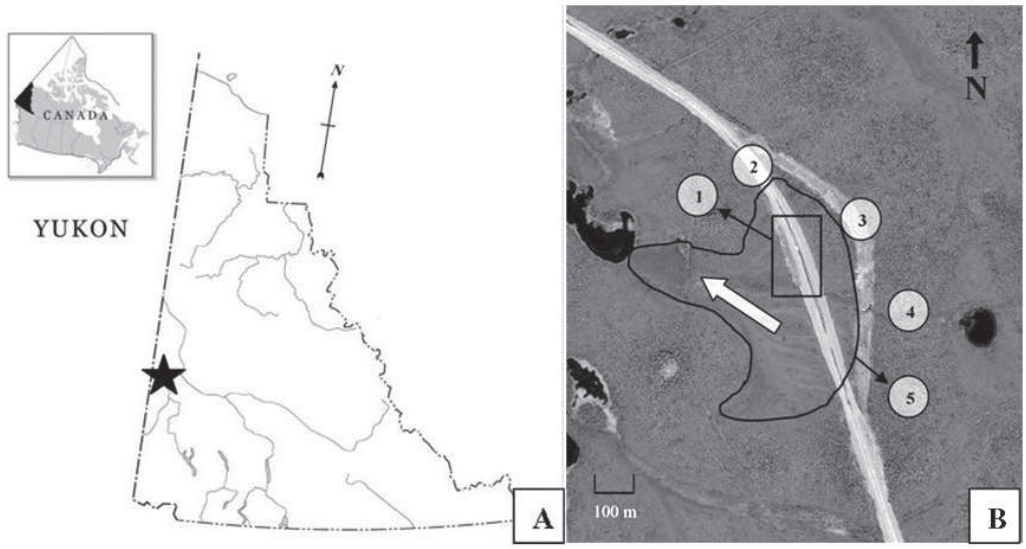

Fig. 3. Groundwater monitoring wells location on each side of the road: (A) eastern side; (B) western side.

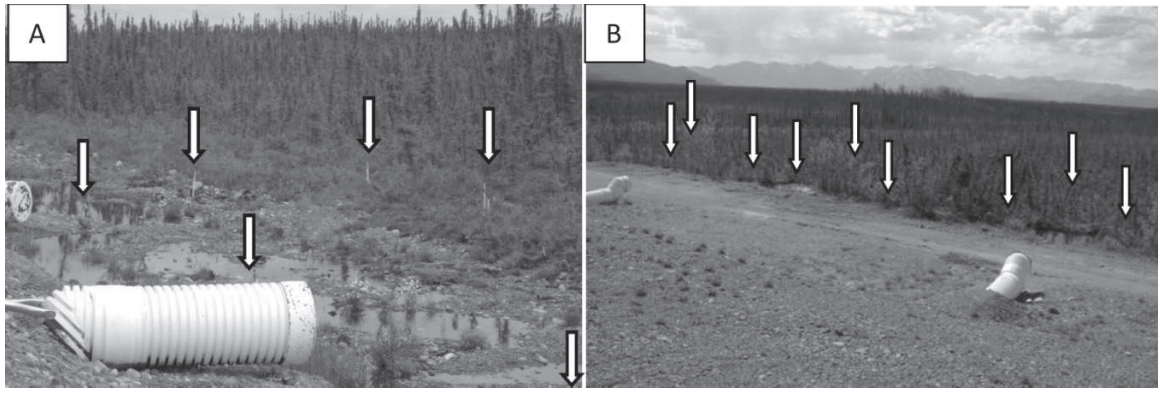

and Jean 1998) to create three-dimensional maps of water-table elevation. Interpolations used the distance weighted method, with 10 neighbors, an exponent of three, and a pixel size of 4 m^2. Flow paths were determined according to these maps.

Topography

The relative elevation between each water observation well was evaluated from a ground survey by optical level (Zeiss Ni2), laser level (Bushnell Rangefinder 1500), and compass. The groundwater monitoring network was referenced to a geodesic benchmark about 100 m from the study site (Natural Resources Canada 2002). The horizontal positions of the wells were determined by a differential global positioning system (DGPS;Trimble GPS Pathfinder Pro XRS with a TSC1 data collector), with a precision of about 0.5 m.

Water well and transect positions were imported into a geographic information system (GIS) and laid over a georeferenced QuickBird (DigitalGlobe, Longmont, Colorado) satellite image of the study site of resolution 0.6 m. Data were integrated in a digital elevation model (DEM) of the study site to view the elevation profile of the study site with a cell dimension of 10 cm.

Temperatures, permafrost table, and thaw depth

Air temperatures were recorded hourly at the study site between October 2008 and December 2010. Other daily climate data (relative humidity, precipitation, and wind) were obtained from Environment Canada's Beaver Creek station, about 8 km northwest of the test site.

Ground temperatures were measured in a 14-thermistor cable installed in 2008 in a borehole drilled through 4 m of embankment material and 12 m of underlying ground on the western side of the road (Fig. 4). Thermistors were housed inside a casing filled with silicone oil to prevent air convection in the hole and provide effective contact with the ground. Temperatures were measured with an accuracy of 0.1 °C between –10 and 10 °C and an accuracy of 0.2 °C through the rest of the operating range (–50 to +30 °C). Data were recorded every 4 hours from October 2008 to October 2010 by a Campbell Scientific CR1000 logger.

Thaw depth was measured beside each groundwater monitoring well in 2008 (October), 2009 (June and August), and 2010 (June and September) by probing and coring. The depth to the permafrost table under the road was estimated by linear interpolation using data from the thermistors at the study

Fig. 4. Digital elevation model (DEM) of the study site showing the road (white stripe), embankment (brown to red stripes), the location of groundwater monitoring wells (green circles for those installed in the natural ground, blue circles for those installed in embankment material, red circles for automatic pressure sensors), and location of thermistor cables (black triangles).

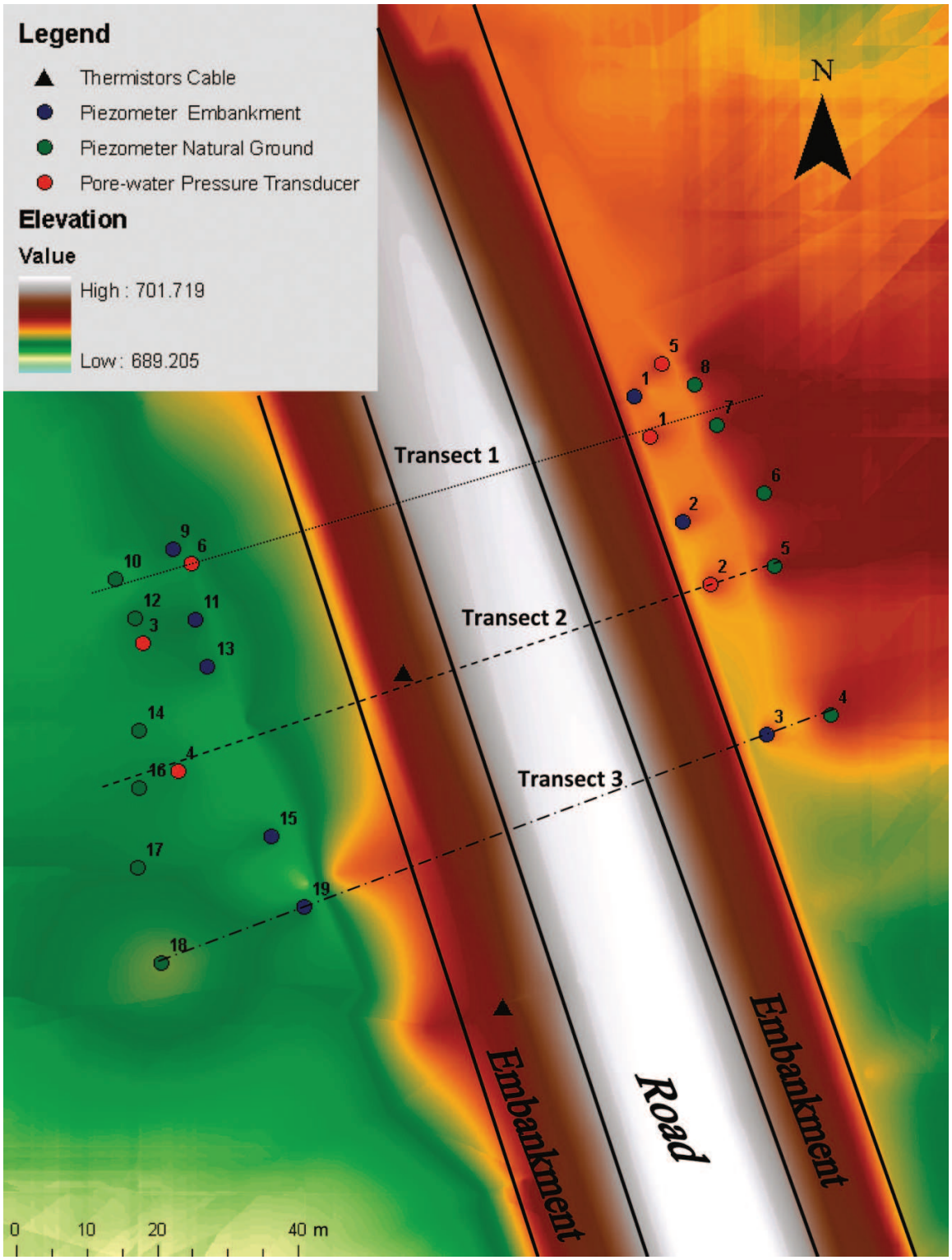

Table 1. Material properties of embankment, peat, and silt used to define waterflow model.

	Material			
Parameters	Embankment	Peat	Silt	Source
Unfrozen soil				
Saturated hydraulic conductivity, K_{sat} (m/s)	1×10^{-4}	8.7×10^{-5}	3×10^{-6}	Field
Residual volumetric water content (m^3/m^3)	0	0	—	Andersland and Ladanyi (2004)
Saturated volumetric water content (m^3/m^3)	0.39	0.81	0.36	Field
In situ volumetric water content (m^3/m^3)	0.39	0.81	0.36	Field
Diameter, 10% passing (mm)	1	—	0.006	Laboratory
Diameter, 60% passing (mm)	10	—	0.06	Laboratory
α^a	—	0.0137	—	Laboratory
n^a	—	1.359	—	Laboratory
Porosity[a]	—	85%	—	Laboratory
m (= 1 – 1/n)[a]	—	0.264	—	Laboratory
Frozen soil				
Saturated hydraulic conductivity, K_{sat} (m/s)	1×10^{-8}	8.7×10^{-8}	3×10^{-8}	Andersland and Ladanyi (2004)
Residual unfrozen volumetric water content (m^3/m^3)	0	—	—	Andersland and Ladanyi (2004)
Saturated unfrozen volumetric water content (m^3/m^3)	0.01	0.01	0.06	Andersland and Ladanyi (2004)

[a]van Genuchten parameter.

Fig. 5. Three-dimensional representation of an interpolation of the natural ground elevation at the study site, with a vertical exaggeration of 5× and a pixel dimension of 2 m × 2 m. The gray circles represent groundwater monitoring wells, and the black dotted lines represent the location of the road. PWPT shows the location of automatic pressure and temperature sensors. The lightest color represents the highest elevation (695 m), and the darkest color represents the lowest elevation (691.5 m).

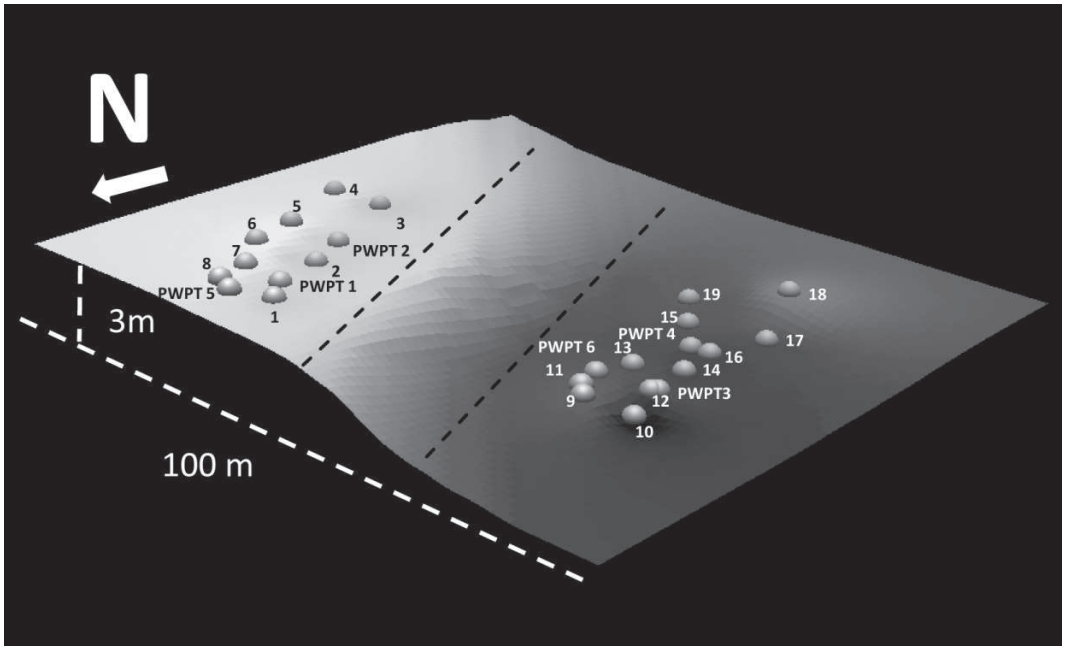

site and others beneath the centerline of the road, about 100 m north and 100 m south of the study section. We assumed active-layer depth was symmetrical about the centerline.

Stratigraphy

Drill cores were described as discussed by Stephani et al. (2010). Cores were also collected beside each groundwater monitoring well with a handheld corer and along three transects each about 100 m long (Fig. 4). Two samples of each layer were taken for grain-size and volumetric water content laboratory analyses according to the procedures D-422 (ASTM 2007) and D-4959 (ASTM 2000). A tension infiltrometer (Decagon mini disk infiltrometer) was used in the laboratory to collect infiltration rate data for each soil sample (three tests per sample). These data were used to calculate the hydraulic conductivity of each soil layer according to the van Genuchten equations (van Genuchten 1980).

Model

A 100 m transect perpendicular to the road (transect 2, Fig. 4) was used to develop a two-dimensional, finite-element groundwater flow model with SEEP/W (GeoStudio version

Fig. 6. Three-dimensional representation of an interpolation of the water-table elevation at the study site, with a vertical exaggeration of 5× and a pixel dimension of 2 m × 2 m. The gray circles represent groundwater monitoring wells, the black dotted lines represent the location of the road, and the black arrows represent flowpaths: (A) 19 June 2009; (B) 11 August 2009; (C) 29 May 2010; (D) 9 September 2010. The yellow color represents the highest elevation (695 m), and the purple color represents the lowest elevation (691.5 m).

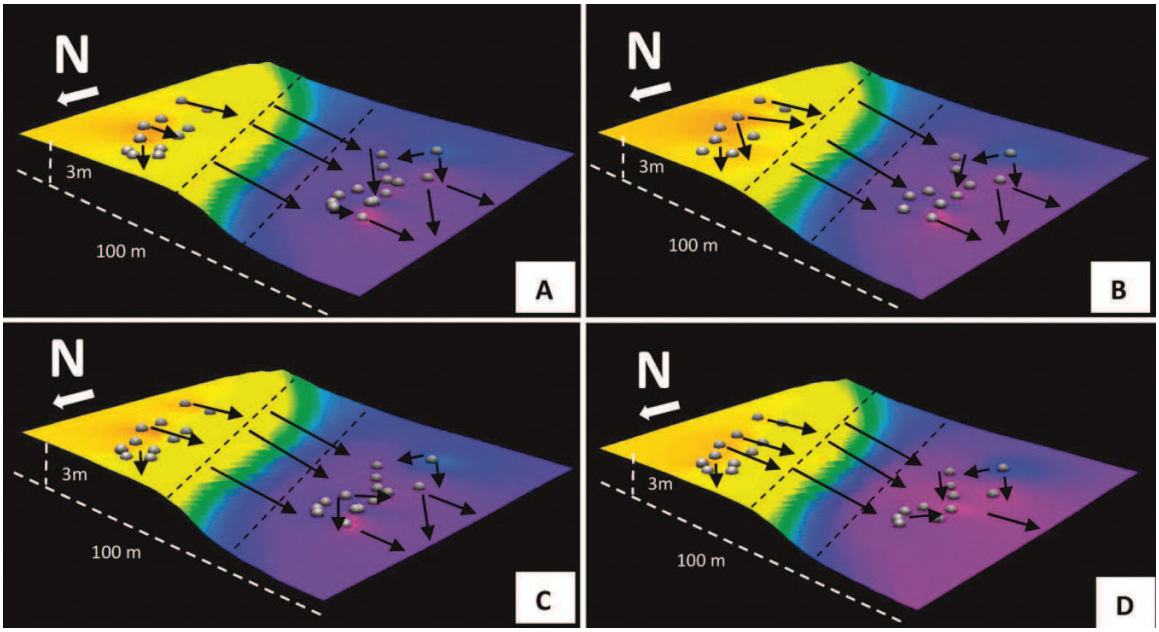

Fig. 7. Water temperatures on the upstream (dotted line) and the downstream side of the road (black line) between May and August 2010.

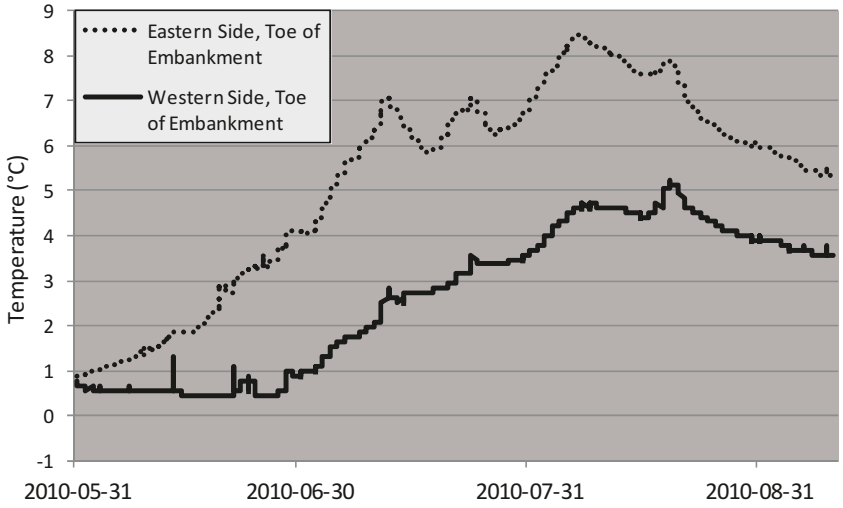

Table 2. Air temperature data for 2009 and 2010.

	2009 (°C)	2010 (°C)
Mean annual air temperature	–3.9	–2.9
Thawing degree-days	1737.8	1719.6
Freezing degree-days	–3153.5	–2768.1
Maxima	31.1	29.9
Minima	–49	–41

7.14, GEO-SLOPE International Ltd., Calgary, Alberta). The model illustrated the evolution of water movement under the road in the embankment material and the natural ground as the position of the permafrost table changed. The model was calibrated with field and laboratory data (Table 1). Groundwater flow simulations were run for 2 years from 1 October 2008, with a time step of 24 h.

Results

Topography and water-table elevation

Figure 4 is a DEM of the study site. The road embankment was about 40 m wide. The edge of the embankment on the eastern side of the road was about 2.5 m higher than the western side. The slope was 2.5% perpendicular to the road. Figure 5 is a DEM of the topography under the road embankment.

Figure 6 shows three-dimensional interpolations of the water table at different times of the year for 2008–2010. The water-table simulations supported our assumption that water was flowing towards and under the road embankment material. Water-table elevation followed the natural topography of the study site and was about 2.5 m lower on the western side of the road than on the eastern side. The difference in water-

Fig. 8. Ground temperatures under the western side slope of the road at the study site. (A) Temperatures from the road surface to the permafrost table. (B) Close-up of the 4.5 m depth where the zero curtain effect is well represented.

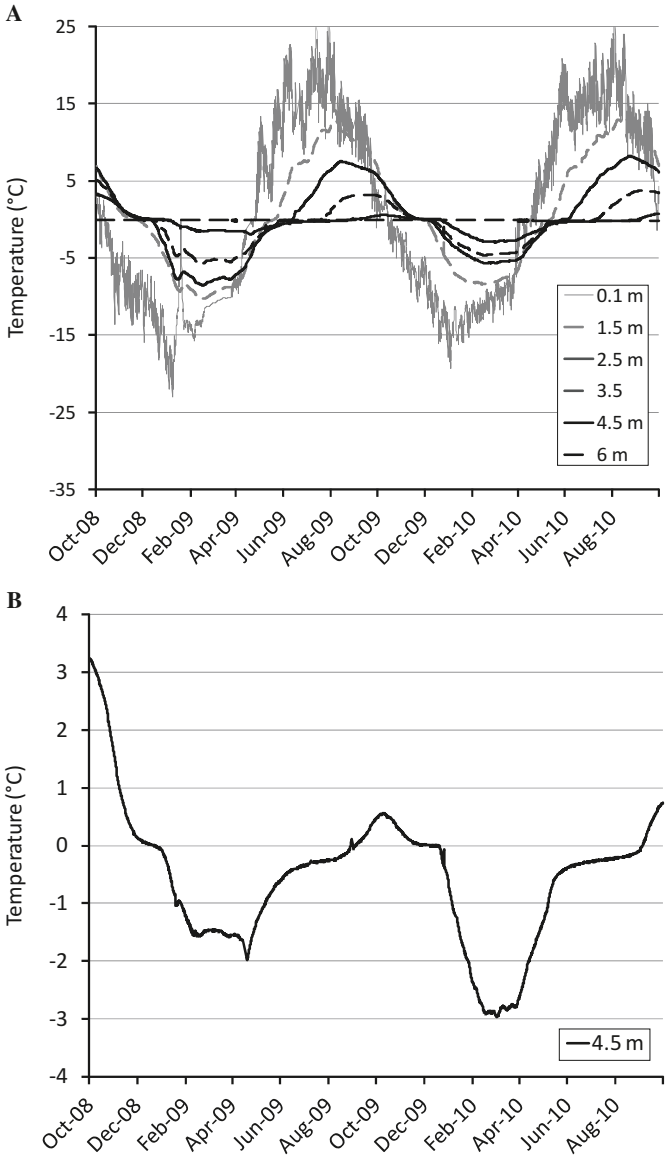

table elevation provided the hydraulic gradient for water flow in the active layer. We assumed that water was flowing from the highest to the lowest point along flow paths estimated from water-table elevation data (black arrows on the figures). Fluctuation of the water table over a year ranged between 10 and 20 cm. Continuous groundwater flow was modeled from snowmelt until complete freeze back of the active layer.

Water temperature

Figure 7 shows water temperatures between May and September 2010 at the toe of the embankment on both sides of the road. Water temperatures on the eastern side were 2–4 °C higher than on the western side in both 2009 and 2010. These data indicate that water was losing heat to the surrounding ground as it flowed under the road.

Air and ground temperature

Air temperature data (mean annual temperature, thawing and freezing degree-days, maxima and minima) for 2009 and 2010 are presented in Table 2. Figure 8A shows ground temperatures from the surface to the permafrost table under the south slope of the embankment. Temperatures were higher, by about 2 °C, at several depths in October 2008 than in 2009 and 2010, due to drilling disturbance. The disturbance dissipated after about 2 months. According to core observations, thermistor data, and linear interpolation of temperatures under the road, the permafrost table was at depths of about 5 m under the side slopes and 6 m under the centerline. The permafrost temperature remained near 0 °C year round from 6 m (–0.1 °C) to 16 m (–0.55 °C) in depth below the road surface. Beside the road, the permafrost table was at a depth of about 90 cm at the toe of the embankment and 70 cm in the undisturbed natural ground away from the embankment.

At a depth of 4.5 m, temperatures remained near 0 °C for an extended period, from June to August and from November to December (Fig. 8B).

Stratigraphy

The stratigraphy of the active layer at the study site comprised peat 30–45 cm thick above cryoturbated peaty silt. The road pavement rested on 4–6.5 m of embankment material (50% gravel, 30% sand, 10% silt) placed on the ground. A drilling campaign in August 2007 revealed an embankment thickness of 6.5 m underneath the centerline of the road. On the side slopes of the road, the embankment was thinner. The ground was unfrozen to about 2 m below the base of the fill.

Grab samples collected from this layer indicated that it was composed of embankment material mixed with saturated peaty silt. This mixture of embankment material and native soil was presumably similar to the material at the toe of the embankment where berms were removed in 2008. Below the 2 m of unfrozen ground, a layer of ice-rich peaty silt extended to about 6.5 m below the natural ground surface. An ice-rich diamicton was observed below 6.5 m. Its total thickness is unknown.

Groundwater flow models

Figure 9 shows a schematic cross section of the road and the underlying undisturbed ground at the study site. To optimize the calculation time and avoid errors due to a complex geometry, the permafrost table was set at a depth of 1 m in the ground beside the road. The permafrost table was set at 6 m under the centerline of the road and at 5 m under the south slope surface. The permafrost table was interpolated between these two points. The groundwater flow model was developed from parameters listed in Table 1.

The computed water table indicates that the water was flowing from the eastern side of the road to the western side (Fig. 10). The ground was saturated year round. Our modeling results suggest that the water table remained roughly constant through the flow season from June to October.

Discussion

Permafrost under the road degraded in part because road construction and maintenance increased heat flow into the

Fig. 9. Cross-sectional transect of the road embankment and the underlying ground in October 2008, with a vertical exaggeration of 2×. White, embankment material (sand and gravel); gray, silt; black, peat. The thick black line represents the permafrost table, and the dotted vertical line represents the location of the thermistor cable above mean sea level (AMSL).

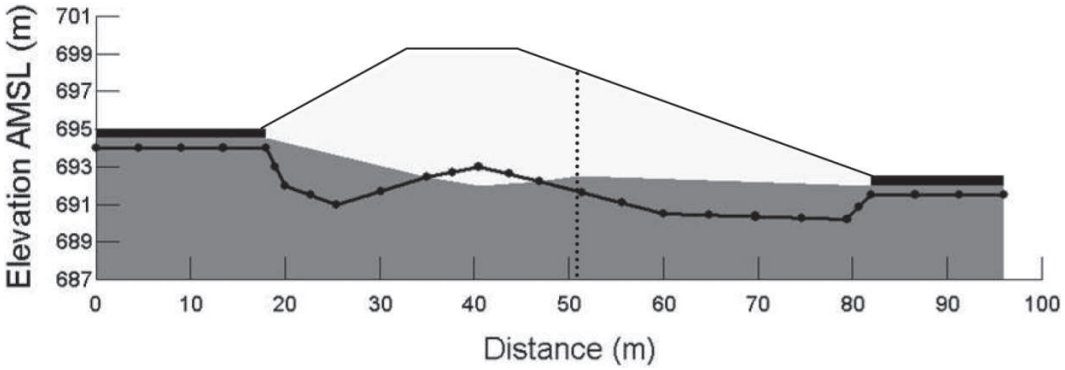

Fig. 10. Simulated water-table elevation (dotted line) on 30 September 2010 on a cross-sectional transect of the road, with a vertical exaggeration of 2×, after 2 years of simulation. White, embankment material (sand and gravel); gray, silt; black, peat. Elevation is given above mean sea level (AMSL).

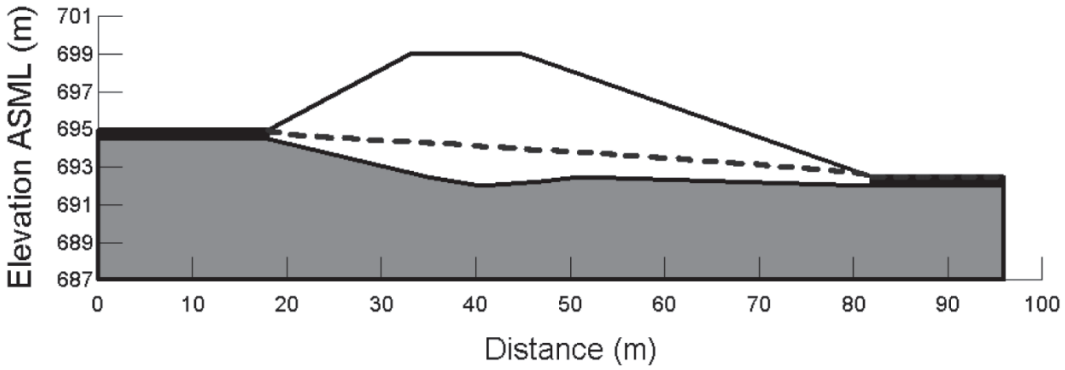

ground. In ice-rich permafrost, the heat supply promoted melting of ground ice, thaw settlement, and road subsidence. As the road subsided over time, the embankment material intercepted the water table where the road crossed the natural drainage pattern. Under the side slopes of the road, the permafrost table was located at about 2 m depth in the underlying ground. The embankment material was thicker under the centerline of the road, and due to the higher thermal conductivity of embankment material, the active layer was thicker.

Groundwater flow modeling and water-table simulations support our hypothesis of water flowing under the road in the active layer and a residual thaw layer. Groundwater flow started in early June on the upstream side of the embankment. The process was accelerated by the presence of unfrozen ground under the slopes of the road. Water flowed first in embankment material, reaching the underlying silt as interstitial ice thawed. In the fall, ground temperatures remained very close to 0 °C between September and November (Fig. 8B). This near isothermal state, called the *zero curtain*, is due to latent heat effects and implies the presence of a large amount of water in the soils beneath the road, retarding freeze back of the embankment. Field observations in October 2009 indicated that groundwater flow continued while the upper part of the active layer was freezing.

Ground temperatures were close to 0 °C year round at the interface of embankment material and silt. Poorly consolidated soils at thawing interfaces, cracks in the ground, macropores along roots, microstructures from freeze and thaw cycles and high unfrozen water content may have raised field hydraulic conductivity of these silts above values determined in the laboratory (Burt and Williams 1976; Mackay 1983). However, the very low hydraulic conductivity of silt likely prevented physically significant discharge. More work remains to be done to quantify the potential groundwater flow in permafrost near 0 °C.

Based on the hydraulic conductivity of material, water took about 5 days to cross the road in embankment in peat material, and about 150 days in silt (assuming no macropores). The rapid response of temperature variations between the upstream and the downstream sides of the road corroborated model results, showing that water was flowing mainly in the high hydraulic conductivity embankment material.

Groundwater flow represented an important source of heat for the ground beneath the road. Temperature measurements showed that water lost heat as it flowed under the road. Groundwater in the embankment material lost heat to the underlying silt, shifting the thermal boundary conditions at the embankment–silt interface. In silt, heat transfers may have melted excess ice, causing an overall increase of hydraulic conductivity in this material upon thawing. The subsequent increase in flow rate likely accelerated advective heat-transfer processes. Reactivation of groundwater flow under the road each summer likely promoted the permafrost degradation which caused the depressions and cracks in the road surface at the study site.

Our findings have practical implications for northern transportation infrastructure. The data suggests that road alignment intersecting groundwater flow paths potentially experience more permafrost degradation than elsewhere. However, more research is needed to compare the ground thermal regimes with and without flowpaths. We demonstrated that permafrost degradation and road subsidence allows for higher thermal conductivity embankment material to sink and intersect the water table. This increases groundwater flow and creates a positive feedback effect that promotes permafrost degradation and additional road subsidence. Our results should be used to develop special road embankment design and mitigation techniques to prevent and accommodate groundwater flow under roads.

Conclusion

The goal of our research was to measure and model the dynamics of groundwater flow interacting with transport infrastructure in discontinuous permafrost. Our results demonstrated that continuous groundwater flow occurred in embankment and silt material under the road at the study site during the thawing period in the summer and during freeze back of the active layer in the fall. The water flow most likely proceeded along preferential flowpaths in the active layer and in unfrozen ground. As water flowed under the road, heat was transferred to the surrounding ground and to the underlying permafrost. Conducto-convective and advective heat transfers induced by groundwater flow likely had a positive feedback on permafrost degradation and probably increased over time as ground ice melted.

The study indicated that groundwater flow should be considered during evaluation of thermal degradation and thaw settlement in saturated discontinuous permafrost terrain. Groundwater flow should also be incorporated in permafrost evolution models and climate-warming scenarios.

Our findings indicate that groundwater flow can have an adverse effect on transportation infrastructure stability. Mitigation techniques also need to be developed to reduce thermal degradation of thaw-susceptible permafrost and resulting destabilization of road embankments.

Acknowledgements

This research was supported by Transport Canada, Yukon Highways and Public Works, the Alaska University Transportation Center, the Natural Sciences and Engineering Research Council of Canada (NSERC), and the Northern Scientific Training Program. Special thanks to the students of the Cold Regions Geomorphology and Geotechnical Laboratory for their help and advice and to Kim Koui (UAF) for his lab and field support. We would also like to thank Dr. Chris Burn for his editorial help, which substantially improved the quality of the manuscript.

References

Andersland, O., and Ladanyi, B. 2004. Frozen ground engineering, second edition. American Society of Civil Engineers & John Wiley & Sons, Inc., Hoboken, NJ.

ASTM. 2000. Standard Test Method for Determination of Water (Moisture) Content of Soil By Direct Heating. ASTM Standard D-4959. ASTM International, West Conshohocken, PA.

ASTM. 2007. Standard Test Method for Particle-Size Analysis of Soils. ASTM Standard D-422. ASTM International, West Conshohocken, PA.

Burt, T.P., and Williams, P.J., 1976. Hydraulic conductivity in frozen soils. Earth Surface Processes, **1**: 349–360.

Daoust, J., and Jean, H. 1998. SIGIS, Geographic Information System and Image Processing. SIGISCO inc. Quebec, Canada. Available from www.sigisco.com [Accessed November 3 2011].

Egginton, P.A., and Dyke, L.D. 1990. Apparent hydraulic conductivities associated with thawing, frost-susceptible soils. Permafrost and Periglacial Processes, **1**(1): 69–77. doi:10.1002/ppp.3430010109.

Environment Canada. 2002. Climatic data of Beaver Creek, Yukon. National Climate Data and Information Archive. Available from www.climat.meteo.gc.ca [Accessed March 7, 2011].

Fortier, R., and Bolduc, M. 2008. Thaw settlement of degrading permafrost: A geohazard affecting the performance of man-made infrastructures at Umiujaq in Nunavik (Québec) *In* J. Locat, D. Perret, D. Turmel, D. Demers and Leroueil, S. 2008. Proceedings of the 4th Canadian Conference on Geohazards: From Causes to Management. Presse de l'Université Laval, Québec, pp. 279–286.

Hinzman, L.D., Bettez, N., Bolton, W.R., Chapin, F.S., Dyurgerov, M.B., Fastie, C.L., et al. 2005. Evidence and implications of recent climate change in northern Alaska and other Arctic regions. Climatic Change, **72**(3): 251–298. doi:10.1007/s10584-005-5352-2.

Jin, H., Zhao, L., Wang, S., and Jin, R. 2006. Thermal regimes and degradation modes of permafrost along the Qinghai-Tibet Highway. Science in China Series D: Earth Sciences, **49**(11): 1170–1183. doi:10.1007/s11430-006-2003-z.

Jorgenson, M., Racine, C., Walters, J., and Osterkamp, T. 2001. Permafrost degradation and ecological changes associated with a warming climate in central Alaska. Climatic Change, **48**(4): 551–579. doi:10.1023/A:1005667424292.

Kane, D., Hinkel, K., Goering, D., Hinzman, L., and Outcalt, S. 2001. Non-conductive heat transfer associated with frozen soils. Global and Planetary Change, **29**(3–4): 275–292. doi:10.1016/S0921-8181(01)00095-9.

Kondratiev, V.G. 2008. Geocryological Problems Associated with Railroads and Highways. *In* Proceeding of 9th International Permafrost Conference, Institute of Northern Engineering, University of Alaska Fairbanks, Fairbanks, AK, pp. 977–982.

Mackay, J.R. 1983. Downward water movement into frozen ground, western arctic coast, Canada. Earth Science, **20**(1): 120–134.

McGregor, R., Hayley, D., Wilkins, G., Hoeve, E., Grozic, E., Roujanski, V., Jansen, A., and Dore, G. 2010. Guidelines for Development and Management of Transportation Infrastructure in Permafrost Regions. Transportation Association of Canada, Ottawa, Ontario.

Natural Resources Canada. 2002. Canadian Spatial Reference System. Available from http://www.geod.nrcan.gc.ca/online_data_e.php [Accessed 3 November 2011].

Natural Resources Canada. 2006. The Atlas of Canada: Yukon. Available from http://atlas.nrcan.gc.ca/site/english/maps/reference/outlineprov_terr/yuk_outline/referencemap_view [Accessed 30 April 2012].

Nelson, F.E., Anisimov, O.A., and Shiklomanov, N.I. 2002. Climate change and hazard zonation in the circum-Arctic permafrost regions. Natural Hazards, **26**(3): 203–225. doi:10.1023/A:1015612918401.

Ogden, A. 2006. Climate, climate change variability and climate change in the Southwest Yukon. Northern Climate Exchange, Whitehorse, Yukon.

Osterkamp, T. 2005. The recent warming of permafrost in Alaska. Global and Planetary Change, **49**(3–4): 187–202. doi:10.1016/j.gloplacha.2005.09.001.

Osterkamp, T., and Romanovsky, V. 1999. Evidence for Warming and Thawing of Discontinuous Permafrost in Alaska. Permafrost and Periglacial Process, **10**(1): 17–37. doi:10.1002/(SICI)1099-1530(199901/03)10:1<17::AID-PPP303>3.0.CO;2-4.

Pullman, E.R., Jorgenson, M.T., and Shur, Y. 2007. Thaw Settlement in Soils of the Arctic Coastal Plain. Alaska. Arctic, Antarctic, and Alpine Research, **39**(3): 468–476. doi:10.1657/1523-0430(05-045)[PULLMAN]2.0.CO;2.

Qingbai, W., Yuanlin, Z., and Yonzhi, L. 2002*a*. Evaluation model of permafrost thermal stability and thawing sensibility under engineering activity. Cold Regions Science and Technology, **34**(1): 19–30. doi:10.1016/S0165-232X(01)00047-7.

Qingbai, W., Yongzhi, L., Jianming, Z., and Chanjiang, T. 2002*b*. A Review of Recent Frozen Soil Engineering in Permafrost Regions along Qinghai-Tibet Highway, China. Permafrost and Periglacial Processes, **13**(3): 199–205. doi:10.1002/ppp.420.

Quinton, W., Shirazi, T., Carey, S., and Pomeroy, J. 2005. Soil Water Storage and Active-layer Development in a Sub-alpine Tundra Hillslope, Southern Yukon Territory, Canada. Permafrost and Periglacial Process, **16**(4): 369–382. doi:10.1002/ppp.543.

Rampton, V. 1971. Late Quaternary Vegetational and Climatic History of the Snag-Klutlan Area, Southwestern Yukon Territory, Canada. Geological Society of America Bulletin, **82**(4): 959–978. doi:10.1130/0016-7606(1971)82[959:LQVACH]2.0.CO;2.

Remchein, D., Fortier, D., Dore, G., Stanley, B., and Walsh, R. 2009. Cost and Constructability of Permafrost Test Sections Along the Alaska Highway, Yukon. *In* Proceedings of Transport Association of Canada Annual Conference, Vancouver, B.C., pp. 1–20.

Scudder, G. 1997. Environment of Yukon *In* Danks and J.A. Downes (*Editors*). Insects of the Yukon. Biological Survey of Canada (Terrestrial Arthropods), Ottawa, Ontario, pp. 13–57.

Smith, S.L., Romanovsky, V.E., Lewkowicz, A.G., Burn, C.R., Allard, M., Clow, G.D., Yoshikawa, K., and Throop, J. 2010. Thermal state of the permafrost in North America: a contribution to the international polar year. Permafrost and Periglacial Processes, **21**(2): 117–135. doi:10.1002/ppp.690.

Stephani, E., and Fortier, D., Shur, Y., Doré, G., and Stanley, B. 2008. Preservation of the Alaska Highway. *In* Proceedings of the 9th International Conference on Permafrost, Institute of Northern Engineering, University of Alaska Fairbanks, Fairbanks, AK. pp. 299–300

Stephani, E., Fortier, D., and Shur, Y. 2010. A cryofacies approach to describe ground ice in permafrost for engineering applications – Case study of a road test site on the Alaska Highway (Beaver Creek, Yukon, Canada). *In* Proceedings of the 6th Canadian Permafrost Conference and 63rd Canadian Geotechnical Conference, Calgary, Alberta. pp. 476–483.

van Genuchten, M. 1980. A Closed-form Equation for Predicting the Hydraulic Conductivity of Unsaturated Soils. Soil Science Society of America Journal, **44**(5): 892–898. doi:10.2136/sssaj1980.03615995004400050002x.

Woo, M., Kane, D.L., Carey, S.K., and Yang, D. 2008. Progress in Permafrost Hydrology in the New Millennium. Permafrost and Periglacial Processes, **19**(2): 237–254. doi:10.1002/ppp.613.